

# Magnetized wake driven anomalous diffusion in complex plasma

Cite as: Phys. Plasmas **28**, 083703 (2021); <https://doi.org/10.1063/5.0055139>

Submitted: 26 April 2021 • Accepted: 23 July 2021 • Published Online: 05 August 2021

 Biswajit Dutta,  Pratikshya Bezbaruah and Nilakshi Das



[View Online](#)



[Export Citation](#)



[CrossMark](#)

## ARTICLES YOU MAY BE INTERESTED IN

[Thermal conductivity of strongly coupled Yukawa fluids](#)

Physics of Plasmas **28**, 084501 (2021); <https://doi.org/10.1063/5.0056763>

[Investigations of the sheath in a dual-frequency capacitively coupled rf discharge by optically trapped microparticles](#)

Physics of Plasmas **28**, 083506 (2021); <https://doi.org/10.1063/5.0057152>

[Effects of a velocity shear on double current sheet systems: Explosive reconnection and particle acceleration](#)

Physics of Plasmas **28**, 082903 (2021); <https://doi.org/10.1063/5.0054501>



Physics of Plasmas  
Features in Plasma Physics Webinars

Register Today!

# Magnetized wake driven anomalous diffusion in complex plasma

Cite as: Phys. Plasmas **28**, 083703 (2021); doi: 10.1063/5.0055139

Submitted: 26 April 2021 · Accepted: 23 July 2021 ·

Published Online: 5 August 2021



View Online



Export Citation



CrossMark

Biswajit Dutta,<sup>1,a)</sup> Pratikshya Bezbaruah,<sup>2</sup> and Nilakshi Das<sup>1</sup>

## AFFILIATIONS

<sup>1</sup>Department of Physics, Tezpur University, Assam 784028, India

<sup>2</sup>Department of Physics, Biswanath College, Assam 784176, India

<sup>a)</sup>Author to whom correspondence should be addressed: [biswaduttajit1995@gmail.com](mailto:biswaduttajit1995@gmail.com)

## ABSTRACT

Diffusion of a three-dimensional dust ensemble embedded in a flowing plasma in the presence of a moderate magnetic field is investigated using Langevin dynamics simulation. It is found that the asymmetric wake potential created due to streaming ions drive the dusty plasma from the subdiffusive to the superdiffusive regime. A novel wake dominant regime is identified that shows superdiffusive behavior for suitable adjustment of the magnetic field. The dependence of the cross field diffusion coefficient on the magnetic field exhibits three distinct behaviors characterized by (a)  $B^{2-3}$  for an ultra-low magnetic field and strongly correlated state, (b)  $B^{>0.1}$  for a moderate magnetic field, and (c) classical  $B^{-2}$  for a relatively large magnetic field. Our analysis shows that the magnetic field is mediated via the streaming ions in regimes (a) and (b) of relatively low magnetic field where the dependence of the diffusion coefficient on the magnetic field is faster than the usual classical regime.

Published under an exclusive license by AIP Publishing. <https://doi.org/10.1063/5.0055139>

## I. INTRODUCTION

The diffusive property of dusty plasma depends on self-diffusion caused by particle–particle interaction as well as collision with background neutral particles. It is an important thermodynamic tool that reflects several important features of a physical system such as inter-particle potential, structural property, and melting or freezing criteria. In the presence of streaming ions and an external magnetic field, the potential around a dust grain may deviate from the Yukawa potential and significantly affect the transport property of the dust ensemble.

In complex plasma laboratory devices, the plasma ions have a flow from the bulk plasma toward the boundaries of the chamber. These flowing ions affect the screening around the dust grains and modify the Debye sphere around the dust particles, introducing anisotropy in the interaction between two dust particles. Because of this, the potential around a dust grain deviates from the isotropic Yukawa potential. The wake potential is the result of accumulation of ions downstream from the dust grains. The resonant interaction between a test dust particle and dusty plasma collective modes gives rise to this oscillatory wake potential. Basically, the ions in the system can exhibit two roles. First, these ions effectively shield the dust grains and give rise to a screened Coulomb potential also known as the Yukawa potential. Second, the drifting ions

(from bulk) are responsible for an overshielding mechanism due to polarization of the background medium by the negatively charged dust grains. These ions distort the symmetric Debye cloud and induce a focusing effect. In the pioneering work by Nambu *et al.*, it was presented that collective effects involving interaction between low-frequency waves in the presence of flowing ions and dust particles levitated in the electrostatic sheath of a plasma chamber give rise to an oscillatory wake potential along the direction of ion flow.<sup>1</sup> Both amplitude and frequency of the potential are further modulated when an external magnetic field acts on such a system.<sup>2–4</sup> Existence of such wake potential has been confirmed by several experimental and simulation works.<sup>3–6</sup> Formation of vertical strings of dust grains along the ion flow direction has been observed, which may be attributed to the attractive, anisotropic wake potential.<sup>7,8</sup> The effect of the wake potential on the behavior of a strongly coupled plasma system has also been studied by several groups. On the other hand, self-diffusion of dust grains has been investigated both in the absence and presence of magnetic field.<sup>9–14</sup> However, the transport property of complex plasma in the presence of magnetized wake potential is not yet fully explored. We try to identify whether ion flow coupled with magnetic field drives the complex plasma to exhibit anomalous diffusion.

The diffusion of dust particles in plasma is a mass transfer effect that results from collisions with other dust particles (self-diffusion), as well as with the background particles, mainly the neutrals. The interparticle interaction between dust grains plays a significant role in controlling the self-diffusion of dust particles. The nature of diffusion of particles can be described using Einstein's formula for mean-squared displacement, defined as  $MSD = \langle |r_i(t) - r_i(0)|^2 \rangle$ , where  $r_i(t)$  is the position of the  $i$ th particle at time  $t$  and the angular bracket denotes an ensemble average. In general,  $MSD(t) \propto t^\alpha$ , where  $\alpha$  is known as the diffusion exponent. Normal diffusion is characterized by  $\alpha = 1$ , while superdiffusion and subdiffusion are characterized by  $\alpha > 1$  and  $\alpha < 1$ , respectively. Both superdiffusion and subdiffusion are also called anomalous diffusion. During the last decade, a number of experiments on diffusion in quasi two-dimensional dusty plasmas have been performed. In many of these, diffusion was found to behave anomalously.<sup>15–17</sup> Ott and Bonitz<sup>18</sup> studied the diffusion of dust grains in strongly coupled plasma (SCP) in the presence of a magnetic field. They have shown the dependence of parallel ( $D_{\parallel}$ ) and perpendicular ( $D_{\perp}$ ) diffusion coefficients on the magnetic field. In the presence of a strong magnetic field, they found Bohm diffusion in strongly coupled regime. With the help of Brownian dynamics simulation, Hou *et al.*<sup>9</sup> analyzed self-diffusion in a two-dimensional dusty plasma system. From the simulation results, they have inferred that the occurrence of superdiffusion is transient and the system exhibits normal diffusion when the Coulomb coupling parameter  $\Gamma$  approaches the melting value. Recently Bezbaruah *et al.*<sup>11</sup> have discussed the effect of screened interaction and ion-neutral collisions on anomalous diffusion of dust grains. In the theoretical work of Ott *et al.*,<sup>19</sup> the system dimension is found to play an important role for superdiffusive behavior. In the experimental work by Liu *et al.*,<sup>20</sup> superdiffusion was found in a two-dimensional dusty plasma liquid that experiences damping due to the background neutrals. In the work, diffusion coefficients are obtained from mean-squared displacement (MSD), and the corresponding scaling with respect to the temperature of the system has been analyzed.

In the present work, we have used Langevin dynamics simulation that takes care of collision with the background neutrals via the frictional damping term due to the neutral particles. The effect of magnetic field and ion streaming velocity is included via the force derived from the relevant wake potential operating among the grains. The sinusoidal dependence of the potential on magnetic field and streaming velocity brings in novel effects to the behavior of diffusion of dust grains. Here, we emphasize that ion flow in the presence of magnetic field perturbs the potential around dust grains. The dielectric response function gets modified and can influence the transport property even for a low value of magnetic field. It is also interesting to investigate the dependence of perpendicular and parallel diffusion coefficient on magnetic field in the presence of Yukawa potential superimposed with anisotropic attractive wake potential. We also try to establish the diffusion coefficient as an indicator of phase transition from ordered to disordered state. The theoretical model and simulation technique are presented in Secs. II and III, respectively. The effects of Coulomb coupling parameter, magnetic field, and ion streaming velocity on diffusion coefficient are discussed in Sec. IV.

## II. THEORETICAL MODEL

We consider negatively charged dust grains embedded in plasma consisting of Boltzmannian electrons, ions, and neutrals. The ions are streaming in the vertical Z-direction perpendicular to an external magnetic field applied along X-direction, as shown in Fig. 1. We are mainly interested in the wake potential that arises due to the interaction between dust grains and electrostatic dust ion cyclotron mode propagating in the system. The dielectric response function for such plasma is given as<sup>3</sup>

$$\epsilon(\omega, k) = 1 + \frac{1}{k^2 \lambda_{De}^2} - \frac{\omega_{pi}^2 k^2}{k^2 (\omega - k \cdot u_{i0})^2 \left( 1 - \frac{\omega_{ci}^2}{(\omega - k \cdot u_{i0})^2} \right)}, \quad (1)$$

In the above equation,  $\omega_{pi}$  is the ion plasma frequency and  $\omega_{ci}$  is the ion cyclotron frequency.

The ions are considered to be magnetized as the transit time of the ions,  $\tau_t = \frac{\lambda_D}{u_{i0}}$  (where  $\lambda_D$  is the screening length provided by the ions,  $u_{i0}$  is the Bohm velocity with which the ions flow), is comparable to the timescale of the cyclotron motion  $\tau_{ci} = \frac{1}{\omega_{ci}}$ . For the parameter regime considered in the present work, the Hall parameter defined as  $H_i = \frac{\omega_{ci}}{\nu_{in}}$  ( $\nu_{in}$  being the ion-neutral collision frequency) exceeds unity so that the effect of ion-neutral collision can be neglected on the ion dynamics and subsequently on the formation of the magnetized wake.<sup>3,21</sup>

Our main focus is on the interaction of dust with the wake in the ion scale so that the effect of dust dynamics on the dielectric response function is not taken into account. The electrons are considered to obey the Boltzmann distribution in the present theory. The deviation from Boltzmann equilibrium is observed in the presence of strong magnetic field in the bulk plasma region. However, the current model is focused to dust grains levitated in the near sheath region where the electrons still follow Boltzmann distribution even in the presence of moderate magnetic field.<sup>22</sup> The electron temperature being sufficiently high ( $10^4$  K), the species get thermalized and behave as classical gas in the ion timescale. Although the effect of ion-neutral collision is found to be

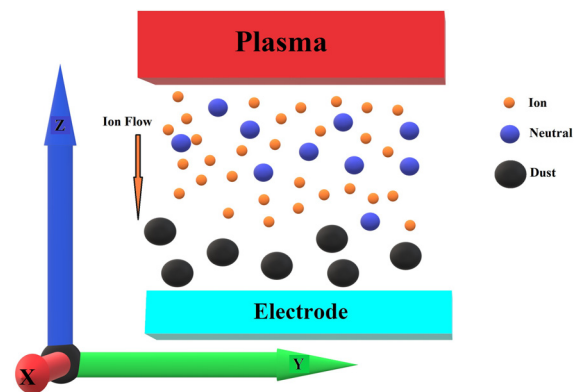


FIG. 1. A 3D dusty plasma with streaming ions and external magnetic field applied along X-direction.

insignificant on the formation of magnetized wake for the parameter regime considered here, the influence of the presence of neutral particle still can play role when we look at the Langevin equation for describing the dust particles. This will be discussed in Sec. III.

The interaction potential among the dust grains in such a condition as derived by Bezbaruah *et al.*<sup>3</sup> is given as

$$\phi = \phi_Y + \phi_W, \quad (2)$$

where  $\phi_Y$  is the Yukawa potential and  $\phi_W$  is the wake potential. The Yukawa potential is given by

$$\phi_Y = \frac{Q_d}{4\pi\epsilon_0 r} \exp\left(-\frac{r}{\lambda_D}\right). \quad (3)$$

Here,  $\lambda_D$  is the Debye screening length ( $\lambda_D = \sqrt{\frac{k_B T_i}{4\pi n_i e^2}}$ ) and  $Q_d$  is the dust charge. The expression for attractive wake potential<sup>3</sup> is given by

$$\phi_W = \frac{-Q_d}{\lambda_{De}\epsilon_0} \frac{\frac{P}{2M^2} \left( -1 + \sqrt{1 + \left(\frac{R}{P}\right)^2} \right) \sin\left( \sqrt{\frac{P}{2M^2} \left( -1 + \sqrt{1 + \left(\frac{R}{P}\right)^2} \right)} z \right)}{\left( \frac{P}{M^2} \sqrt{1 + \left(\frac{R}{P}\right)^2} \right) \left[ \frac{P}{2M^2} \left( -1 + \sqrt{1 + \left(\frac{R}{P}\right)^2} \right) + 1 \right]}. \quad (4)$$

Here,  $M = \frac{u_{i0}}{\omega_{pi}\lambda_{De}}$  is the Mach number,  $f_i = \frac{\omega_{di}}{\omega_{pi}}$  is the normalized ion gyro frequency,  $u_{i0}$  is the ion drift velocity,  $\omega_{pi}$  is the ion plasma frequency,  $\omega_{ci}$  is the ion cyclotron frequency,  $P = M^2 - f_i^2 - 1$  and  $R = 2Mf_i$  are two normalized parameters. The nature and behavior of the potential have been analyzed in detail in that work. The theoretical model was developed under the assumption  $k_{\parallel}^2 \gg k_{\perp}^2$ , where  $k_{\parallel}$  is the parallel (to the direction of ion flow) component of wave vector and  $k_{\perp}$  is the perpendicular (to the direction of ion flow) component of wave vector. This approximation is intimately connected with the neglect of EB drift.<sup>23</sup> For the chosen parameter regime, the ion flow due to electrostatic sheath dominates over the EB drift in the perpendicular direction. This is true when  $\frac{k_{\parallel}^2}{k_{\perp}^2} \gg \frac{u_{d0}}{u_{i0}}$ , where  $u_{d0}$  is the unperturbed EB drift of ions and  $u_{i0}$  is the unperturbed ion drift velocity due to electrostatic sheath.

The amplitude and phase of this asymmetric wake potential obtained in the ion flow direction are controlled by two important parameters, i.e., Mach number (M) and magnetic field (B). The particle-wake interaction and interplay with the magnetic field and different ion flow speeds are also discussed in detail. The pressure exerted by neutral density used in the simulation of dust motion is low enough that the effect of ion-neutral collision can be neglected on the formation of wake. Using this potential, the combined role of wake and Yukawa potentials on dust diffusion process as a characteristic of different ion flow speeds and magnetic fields have been investigated using Langevin dynamics simulation.

### III. SIMULATION SCHEME

The calculation of transport coefficients is one of the most powerful applications of molecular dynamics simulations. The equilibrium methods, make use of the Helfand–Einstein or the Green–Kubo relations to obtain information about the transport process from systems in thermodynamic equilibrium. Langevin dynamics simulation has been performed for 864 dust particles, with an additional Lorentz force acting on dust particles due to the external magnetic field. In this

simulation scheme, for each particle  $i$ , the Langevin equation has been integrated,

$$\ddot{r}_i(t) = \frac{Q_d(\dot{r}_i(t) \times B)}{m_d} - (1/m_d) \nabla \sum_{j \neq i} \phi_{ij} - \nu \dot{r}_i(t) + \frac{1}{m_d} \zeta(t). \quad (5)$$

Here,  $Q_d(\dot{r}_i(t) \times B)$  is the Lorentz force,  $\nu \dot{r}_i(t)$  is the frictional drag, which appears due to the dust particles motion in surrounding buffer plasma.  $\nu$  is a friction coefficient, which is associated with the frequency of the dust particle collisions with the buffer plasma particles, and  $\zeta(t)$  is the random force which is assumed to have a Gaussian distribution.<sup>24</sup>  $\phi_{ij}$  is the inter-particle potential energy of the dust particles.  $\phi_{ij}$  takes account of all the possible interactions between dust grains. The behavior of the system is controlled by the dimensionless parameters which are  $\Gamma = \frac{Q_d^2}{4\pi\epsilon_0 n_i K_B T_d}$ ,  $\kappa = \frac{r_{av}}{\lambda_D}$ ,  $M = \frac{u_{i0}}{\omega_{pi}\lambda_{De}}$ , and  $f_i = \frac{\omega_{di}}{\omega_{pi}}$ . The particles are assumed to interact via isotropic Yukawa potential, defined as  $\phi_Y = \Gamma \kappa \frac{\exp(-r)}{r}$ , and anisotropic asymmetric ion flow induced wake potential which is given by Eq. (4). This asymmetric wake potential comes into play along the direction of ion flow (z-direction). In our simulation, time and length are normalized by  $\sqrt{\frac{m_d \lambda_D^2}{K_B T_d}}$  and  $\lambda_D$ , respectively. In the simulation, parameters related to dust grains are dust mass  $m_d = 10^{-15}$  Kg, dust particle radius  $r_d = 10^{-6}$  m, and dust grain density  $n_d = 10^{11} \text{ m}^{-3}$ .

We start with a total of 864 (say N) particles in a cubical simulation box of size  $L_x = L_y = L_z = 10^{-3}$  m (volume,  $V = L_x L_y L_z$ ) initially distributed in a face-centered cubic (fcc) lattice containing four dust particles per unit cell. The initial state is prepared by first connecting the system to a Berendsen thermostat. The temperature fluctuations are regulated through velocity re-scaling with the use of this Berendsen thermostat.<sup>24</sup> We have implemented periodic boundary conditions so that the particle number in the system is conserved during the time of simulation. The equation of motion has been solved using velocity Verlet algorithm.<sup>24</sup> The simulation is performed in the following steps: (i) canonical (NVT) run: first we perform a canonical

ensemble simulation to take the system to a thermal equilibrium at required  $\Gamma$  by connecting it to the Berendsen thermostat. (ii) Microcanonical (NVE) run: after step (i), we remove the thermostat and perform a microcanonical ensemble simulation to bring the system to the desired equilibrium. All the required equilibrium properties have been calculated during the microcanonical run (where the number of particles, the volume of the system, and the total energy are conserved) after the system attains equilibrium.

The structural behavior of the dust grains is investigated on the basis of radial distribution function  $g(r)$  defined as

$$g(r) = \frac{V N(r, dr)}{N 4\pi r^2 dr}, \quad (6)$$

where  $V$  is the volume of the simulation box and  $N(r, dr)$  is the number of particles in the shell with infinitesimal thickness  $dr$ . The nature of diffusion in the system of particles is described using Einstein's formula with the help of mean-squared displacement defined as

$$MSD(t) = \frac{1}{N} \sum_{i=1}^N (r_i(t) - r_i(t_0))^2, \quad (7)$$

where  $r_i(t)$  is the position of the  $i$ th particle at time  $t$ . In general,  $MSD(t) \propto t^\alpha$  where  $\alpha = 1$  for normal diffusion,  $\alpha < 1$  is for subdiffusion and  $\alpha > 1$  is for superdiffusion. The components of diffusion coefficient, parallel and perpendicular to the magnetic field are defined as

$$D_{\parallel} = \lim_{t \rightarrow \infty} \frac{\langle |x(t) - x(t_0)|^2 \rangle}{2t}, \quad (8)$$

$$D_{\perp} = \lim_{t \rightarrow \infty} \frac{\langle |y(t) - y(t_0)|^2 \rangle + \langle |z(t) - z(t_0)|^2 \rangle}{4t}. \quad (9)$$

Here, the angular brackets represent the averaging of displacement square over the entire ensemble of particles. The phase behavior and structural properties have been analyzed by the radial distribution function  $g(r)$ ,<sup>24</sup> Lindemann parameter (defined as  $\frac{\sqrt{MSD}}{r_{av}}$ ),<sup>25</sup> and lattice correlation factor (which is the Fourier transform of the radial distribution function).<sup>24</sup>

#### IV. RESULTS AND DISCUSSION

Here, we report some results on self-diffusion of charged dust particles in the presence of an external magnetic field and ion flow. The diffusion property of dust grains in the present work is mainly controlled by Coulomb coupling parameter  $\Gamma$ , screening parameter  $\kappa$ ,

normalized ion flow velocity, i.e., Mach number  $M$ , magnetic field  $B$ , and dissipation arising from neutral pressure.

In order to understand the nature of transport of a driven, dissipative dusty plasma system as discussed above, we perform several sets of Langevin dynamics simulation for a wide range of values of Coulomb coupling parameter  $\Gamma$ , screening parameter  $\kappa$ , normalized ion flow velocity, i.e., Mach number ( $M$ ), and magnetic field ( $B$ ). MSD is plotted against time in Figs. 2(a) and 2(b) in linear and logarithmic scales, respectively, for values of  $\Gamma$  ranging from 45 to 370 keeping neutral density  $n_n$  at  $10^{21} \text{ m}^{-3}$ ,  $B = 0.001 \text{ T}$ ,  $\kappa = 2$ , and  $M = 1.9$ . MSD values decrease with an increase in the Coulomb coupling parameter  $\Gamma$  as expected.<sup>9</sup> In order to understand the nature of diffusion of the dusty plasma system, the diffusion exponent  $\alpha$  is obtained in Fig. 2(b) from the slope of MSD vs time graph on the log-log scale [ $MSD(t) \propto t^\alpha$ ]. For normal diffusion,  $\alpha$  is equal to unity, whereas for anomalous diffusion,  $\alpha > 1$  (superdiffusion) or  $\alpha < 1$  (subdiffusion).<sup>18</sup> The system undergoes subdiffusion in the entire time of observation, since  $\alpha < 1$ .

Figures 2(c<sub>1</sub>)–2(c<sub>4</sub>) are the radial distribution functions [ $g(r)$ ] depicting the variation in grain ordering for different values of  $\Gamma$ . A transition from fluid to solid crystalline state is admitted on increasing the value from  $\Gamma = 45$  to  $\Gamma = 370$  [Figs. 2(c<sub>1</sub>)–2(c<sub>4</sub>)]. The appearance of multiple peaks in  $g(r)$  plots indicate a transition from disordered to ordered solid like state with reduction in MSD values. Increase in coupling parameter is responsible for strong correlation among particles by counteracting the anisotropy arising due to ion flow. Our primary interest is to see whether the diffusion property of complex plasma can be controlled by tuning the amplitude and frequency of the magnetized wake.

The Lorentz force  $Q_d(\dot{r}_i(t) \times B)$  acting on dust grains is negligibly small due to the small charge to mass ratio of dust grains, and the magnetic field manifests itself, mainly through the wake potential for the weak to moderate values of magnetic field considered here. This is evident from the comparison of  $g(r)$  plots of Figs. 3(a<sub>1</sub>)–3(a<sub>4</sub>) and 3(b<sub>1</sub>)–3(b<sub>4</sub>), respectively. Figures 3(a<sub>1</sub>)–3(a<sub>4</sub>) depict the results when the simulation was performed with Yukawa potential only along with the Lorentz force term. The system remains in crystalline state when  $B$  is varied from 0.001 to 0.09 T in this case. On the other hand, when wake potential is included, one observes transition from solid crystalline to gaseous state [Figs. 3(b<sub>1</sub>)–3(b<sub>4</sub>)].

The effect of the magnetized wake on MSD when  $B$  is varied from 0.001 to 0.1 T is shown in Figs. 4(a) and 4(c). The values of

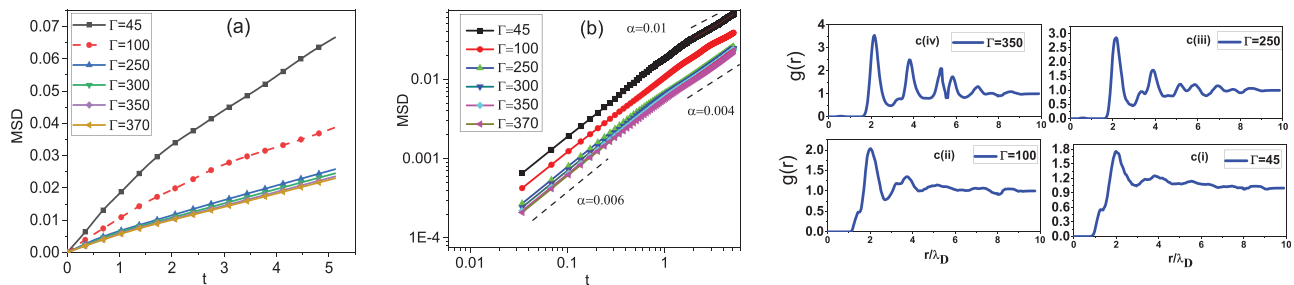


**FIG. 2.** (a) Mean-squared displacement (MSD) for a range of  $\Gamma$  values when  $B = 0.001 \text{ T}$ ,  $\kappa = 2$ ,  $M = 1.9$ , and  $n_n = 10^{21} \text{ m}^{-3}$ . In our simulation, both MSD and time are normalized. Time and length are normalized by  $\sqrt{\frac{m_d \lambda_D^2}{k_B T_d}}$  and  $\lambda_D$ , respectively. Figure 2(b) is the result of fitting the MSD time series of Fig. 2(a) in a log-log plot (logarithmic scale) to find the value of diffusion exponent  $\alpha$  for different values of coupling parameter. (c) The plot of radial distribution functions [ $g(r)$ ] depicting the variation in grain ordering for different values of  $\Gamma$ .



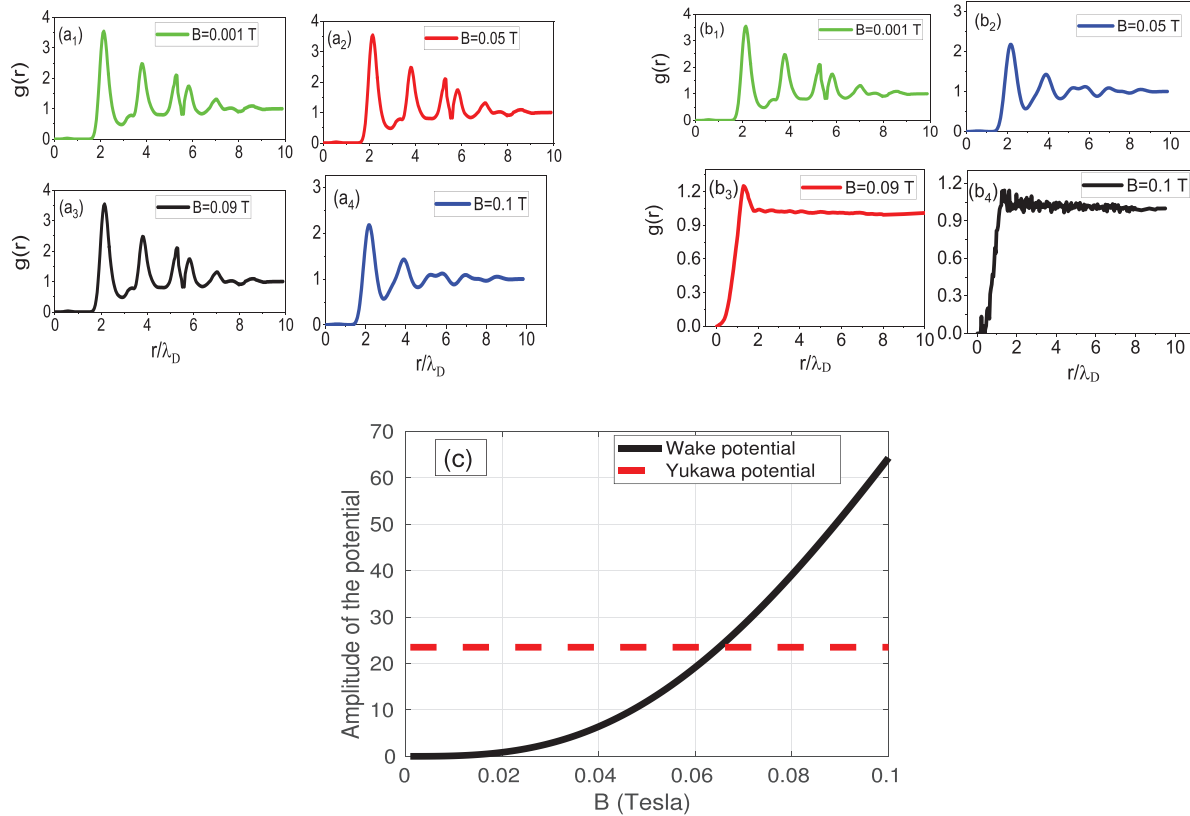


**FIG. 3.** (a<sub>1</sub>)–(a<sub>4</sub>) are the plots of  $g(r)$  depicting the variation in grain ordering for different values of  $B$  when  $\Gamma = 350$ ,  $\kappa = 2$ ,  $M = 1.9$ , and  $n_n = 10^{21} \text{ m}^{-3}$ ; the simulation was performed with Yukawa potential only along with the Lorentz force term. (b<sub>1</sub>)–(b<sub>4</sub>)—plots of  $g(r)$  for different values of  $B$  considering both Yukawa and magnetized wake potential. (c) Comparison of the amplitude of wake and Yukawa potential in the ion flow direction.

neutral density  $n_n$ , coupling parameter  $\Gamma$ , screening parameter  $\kappa$ , and ion Mach number  $M$  are kept fixed at  $10^{21} \text{ m}^{-3}$ , 350, 2, and 1.9, respectively. As the magnetic field is changed from 0.001 to 0.1 T, the dust ensemble exhibits an increase in MSD values. The diffusion exponents are calculated from the slope of MSD curves in the log–log plots of Fig. 4(b), Fig. 4(c), and plotted across  $B$  in Fig. 4(d). The plots reveal that as the magnetic field is increased from 0.001 T, the dust ensembles gradually transit to a disordered state. It makes a transition to liquid state at magnetic field around 0.05 T. The lattice correlation factor (LCF) is 0.45 for  $B = 0.05$  T. At this value of magnetic field ( $B = 0.05$  T), there is also a change in the slope of Lindemann parameter [Fig. 4(e)]. This signifies a change in the phase behavior due to the magnetic field. With the increase in  $B$ , the diffusion exponent is enhanced indicating a transition from subdiffusion to superdiffusion. Both MSD and the values of diffusion exponent  $\alpha$  exhibit a sudden change in the slope around magnetic field  $B = 0.05$  T. These observations can be explained on the basis of the plot of wake potential as shown in Fig. 4(f). Both the amplitude and frequency of the wake potential ( $\phi_w$ ) increase with an increase in the value of  $B$ . An increase in the strength of magnetic field facilitates the focusing of ions flowing from bulk to the sheath region below the dust grains, thus enhancing the density of trapped ions, resulting in an increase in the amplitude of the wake potential. This anisotropic potential acting along ion flow direction is responsible

for the observed increase in MSD values and diffusion exponent. It can be inferred that by suitably tuning the magnetic field, it is possible to design a dust ensemble which is subdiffusive or superdiffusive in its behavior.

Perpendicular and parallel diffusion coefficients are plotted across  $B$  in Figs. 5(a) and 5(b), respectively. Due to the presence of magnetized wake, MSD shows strong dependence on  $B$  even for its low values. A complete novel characteristic of transport of dust ensemble is observed for  $0.001 \text{ T} < B < 0.01 \text{ T}$  keeping  $M$  fixed at 1.9 where the decay exponent  $\gamma$  (defined as  $D_{\perp} \propto B^{\gamma}$ ) is found to be  $> 2$ . This result is in contrast with the previous findings where cross field diffusion remains indifferent to variation in  $B$  in this regime.<sup>18</sup> We emphasize that such weak magnetic field does not affect dust particles via Lorentz force, rather manifests through the modification in background plasma response function. The novel behavior of diffusion coefficient may be explained on the basis of a symmetry breaking caused by flowing magnetized ions. The magnetic field is not too strong in this regime to confine the dust particles, but sufficient to affect the wake formed behind dust grains. The magnitude of effective potential gradually moves from Yukawa dominant to wake dominant, thus resulting in enhancement of MSD and decay exponent. Figure 3(c) shows the comparison of the amplitudes of wake and Yukawa potential in the ion flow direction. As we increase the magnetic field from 0.001

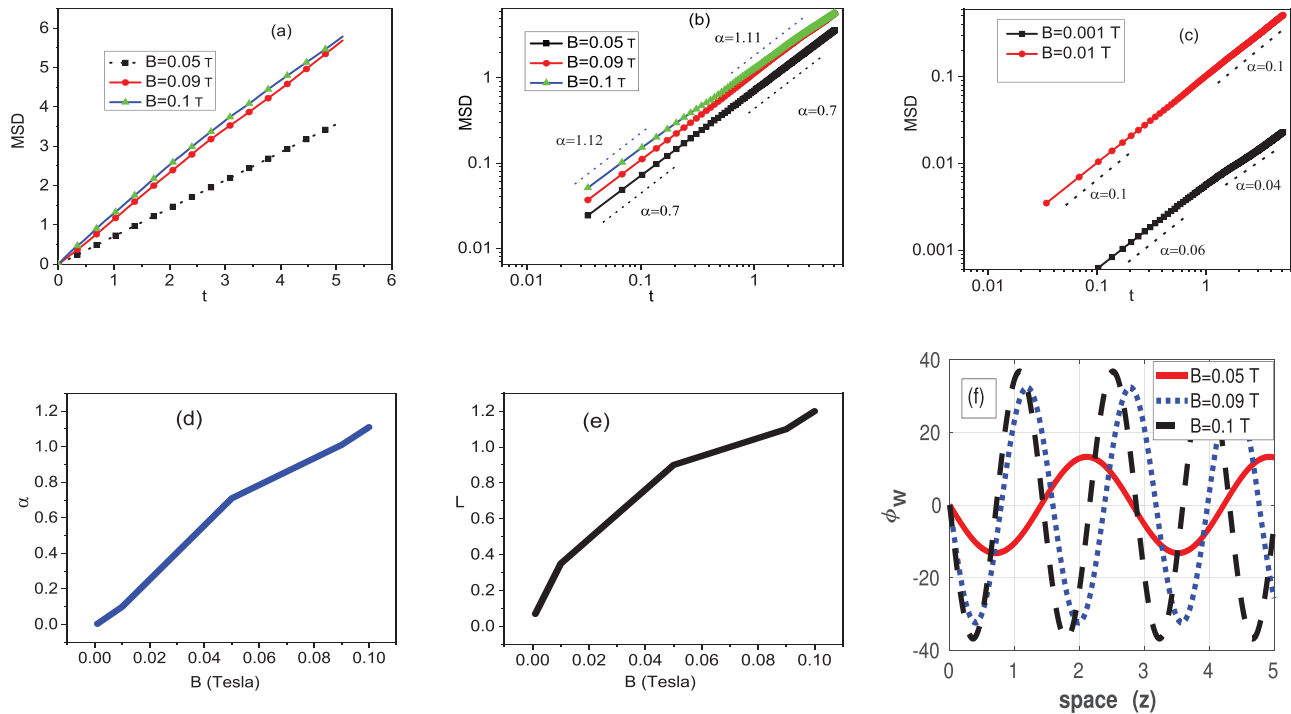


**FIG. 4.** (a) The figure depicts the evolution of MSD for a range of  $B$  values when  $\Gamma = 350$ ,  $\kappa = 2$ ,  $M = 1.9$ , and  $n_n = 10^{21} \text{ m}^{-3}$ . (b) and (c) MSD in the log-log plot as a function of time. (d) The diffusion exponent ( $\alpha$ ) for different values of field strengths. (e) Shows the effect of magnetic field ( $B$ ) on the Lindemann parameter. (f) Shows the variation in the strength of wake potential ( $\phi_W$ ) for a set of magnetic field.

to 0.1 T, the wake potential gradually increases and exceeds Yukawa. The trend is reversed beyond 0.09 T. The cross field diffusion coefficient ( $D_{\perp}$ ) now decreases with  $B$  exhibiting a negative slope. This is also the regime, where the system goes to a disordered state exhibiting superdiffusion. In this regime, the Lorentz force term starts to become effective and shows its influence on diffusion property of the system. Moreover, wake potential becomes dominant in this range of magnetic fields and causes the dislocation of dust particles from the ordered state. This result is in agreement with the findings of Ott and Bonitz.<sup>18</sup> They observed that for small values of  $\Gamma$ , i.e., in the weakly

coupled regime, magnetic field suppresses the cross field diffusion. However, in our simulation, we observe that combination of Lorentz force and magnetized wake results in  $\frac{1}{B^2}$  dependence of cross field diffusion coefficient instead of Bohm diffusion. From this analysis, the dependence of  $D_{\perp}$  on magnetic field may be classified into three regimes: (a) a novel regime, characterized by solid like state, ultra-low magnetic field ( $B < 0.01 \text{ T}$ ) where  $D_{\perp} \propto B^{\gamma}$  with  $\gamma > 2$ . In this regime, even a small change in magnetic field results in large deviation from Yukawa potential due to increase in asymmetric wake potential. Here transport of particles are found to be subdiffusive. It is worth noting

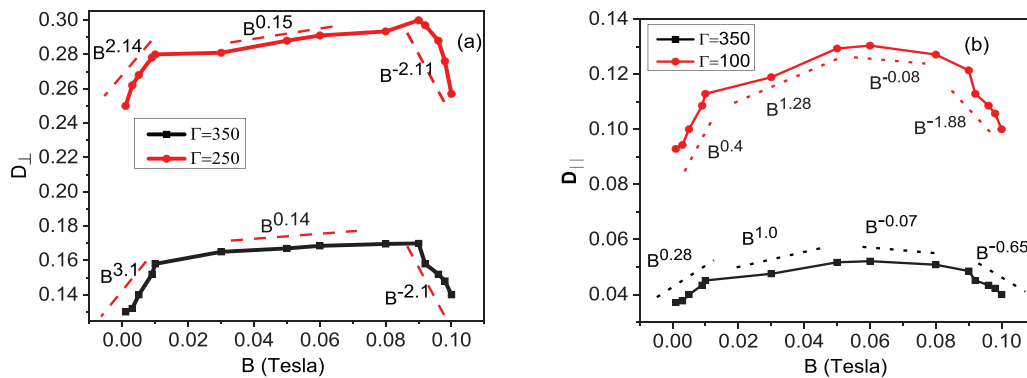


**FIG. 5.** Diffusion coefficients (a) perpendicular ( $D_{\perp}$ ) and (b) parallel ( $D_{\parallel}$ ) to the magnetic field vs field strength ( $B$  in Tesla) for a range of coupling parameter when  $\kappa = 2$ ,  $M = 1.9$ , and  $n_n = 10^{21} \text{ m}^{-3}$ .

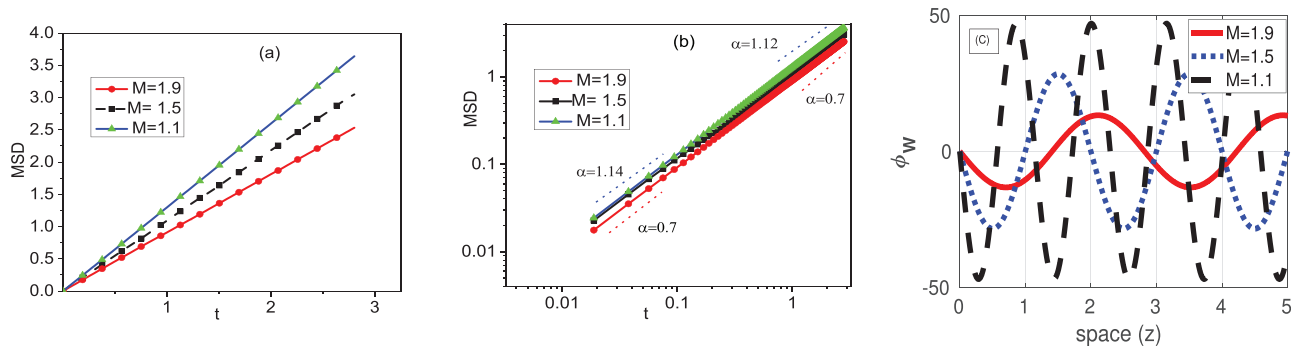


**FIG. 6.** (a) The figure depicts the evolution of MSD for a range of  $M$  values when  $B = 0.05$  T,  $\Gamma = 350$ ,  $\kappa = 2$ , and  $n_n = 10^{21} \text{ m}^{-3}$ . (b) The straight line fit of the MSD curve is represented through the dashed lines in the figure. (c) The variation in strength of wake potential ( $\phi_w$ ) for a set of Mach number for  $B = 0.05$  T,  $\Gamma = 350$ ,  $\kappa = 2$ , and  $n_n = 10^{21} \text{ m}^{-3}$ .

that the effect of magnetic field in this regime is mediated purely by flowing ions and not due to usual Lorentz force on plasma particles. (b) a plateau region where  $D_{\perp} \propto B^{-0.1}$  for  $0.01 \text{ T} < B < 0.09 \text{ T}$ . (c) a classical region where  $D_{\perp} \propto B^{-2}$ . In this regime, diffusion is the result of combined action of Lorentz force and strong wake potential. Variation of parallel diffusion with  $B$  is shown in Fig. 5(b). Parallel diffusion is weak in comparison to perpendicular diffusion. It increases with  $B$  up to  $0.05 \text{ T}$  beyond which, it shows a negative slope. The change in slope occurs at a magnetic field that coincides with a point of transition from crystalline to liquid state. Like cross field diffusion,  $D_{\parallel}$  also further gets suppressed beyond  $B = 0.09 \text{ T}$ . In the work by Ott and Bonitz,<sup>18</sup> parallel diffusion is found to remain indifferent for low values of magnetic field. In contrast, here we observe a significant increase in  $D_{\parallel}$  for very weak magnetic field which is attributed to the influence of magnetized wake.

It is the ion flow velocity that drives the attractive oscillatory wake potential and modulates its amplitude and velocity as shown in Fig. 6(c). The results of MSD with time for a range of normalized ion flow velocity in the supersonic regime are illustrated in Figs. 6(a) and 6(b) for  $B = 0.05 \text{ T}$ ,  $\kappa = 2$ , and  $\Gamma = 350$ . With an increase in the value of  $M$ , the orderliness of the dust ensemble increases and MSD values gradually decrease. The ion focusing gets distorted as the velocity of

flowing ions increases. As a result, the strength of wake potential becomes weaker and Yukawa potential becomes more dominant. This results in a stronger correlation among the grains and MSD values decrease. The plot of diffusion exponent with  $M$  in Fig. 7(a) brings out some interesting properties of diffusion shown by the system. The values of  $\alpha$  indicate super-diffusion for  $1.0 < M < 1.2$ ; whereas  $\alpha$  decreases to subdiffusion beyond  $M = 1.2$  and shows an abrupt change in slope at  $M = 1.5$ . In order to understand the mechanism behind the transition from super-diffusion to subdiffusion, we have calculated the spring constants from the expression of potentials. The spring constant is defined as  $K = \frac{d^2\phi}{dr^2}$ , where,  $\phi$  is the effective potential as a function of the distance  $r$ . The effective spring constant along the direction of ion flow is  $K_z = K_z(\text{Yukawa}) + K_z(\text{wake})$ . The spring constant gives an idea about the strength of dominant interaction operating in the system. It is clearly seen from Fig. 7(b) that effective spring constant  $K_z$  shows a dip corresponding to  $M = 1.1$  and this means that attractive wake potential dominates over repulsive Yukawa potential. This increases the disorderliness of the system and drives the system to exhibit superdiffusion. As  $M$  increases beyond  $1.2$ , Yukawa potential dominates over wake and the system goes to subdiffusive regime. Around  $M = 1.5$ , Yukawa becomes maximum and brings in regularity to the system and diffusion beyond this almost becomes steady.

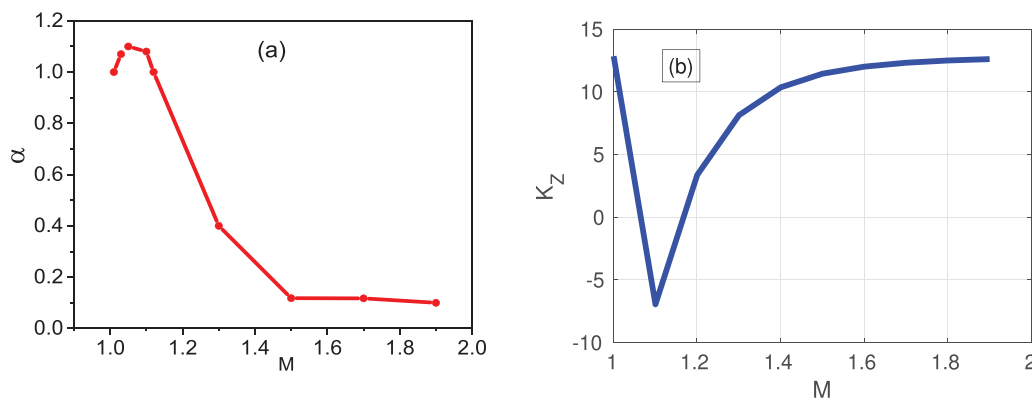


**FIG. 7.** (a) Diffusion exponent  $\alpha$  vs  $M$  when  $B = 0.05 \text{ T}$ ,  $\Gamma = 350$ ,  $\kappa = 2$ , and  $n_n = 10^{21} \text{ m}^{-3}$  (b) Effective spring constants  $K_z$  vs  $M$  for  $B = 0.05 \text{ T}$ ,  $\Gamma = 350$ ,  $\kappa = 2$ , and  $n_n = 10^{21} \text{ m}^{-3}$ .



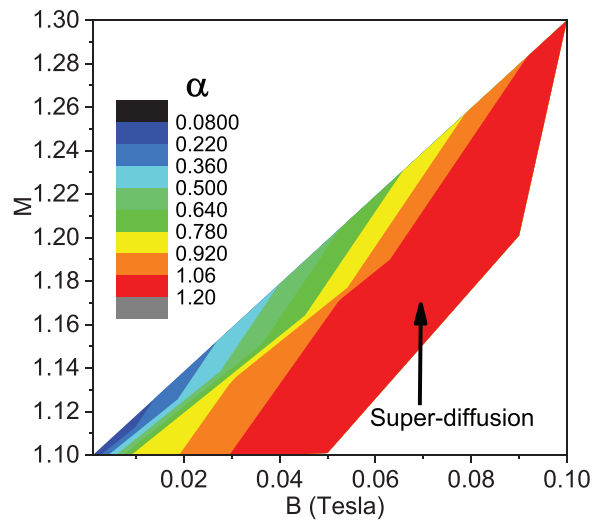


**FIG. 8.** Diffusion exponent  $\alpha$  as a function of magnetic field strength ( $B$  in Tesla) and Mach number ( $M$ ) for  $\Gamma = 350$ ,  $\kappa = 2$ , and  $n_n = 10^{21} \text{ m}^{-3}$ .

Figure 8 depicts the range of Mach number ( $M$ ) and magnetic field ( $B$ ) for which the dust ensemble exhibits superdiffusion. The red region as indicated in the figure represents superdiffusion ( $\alpha > 1$ ). The simulation performed in this work clearly reveals that superdiffusive property is exhibited when effective potential becomes wake dominant. The asymmetric wake potential drives the dust ensemble toward a disordered and superdiffusive state.

## V. CONCLUSIONS

The perturbation of the Debye sphere around the dust grains due to the streaming magnetized ions modifies the dielectric response of the plasma medium and leads to the appearance of a new anisotropic interaction potential. In most of the previous work, the effect of magnetic field on diffusive properties of dusty plasma was investigated via the influence of the Lorentz force. Due to small charge to mass ratio, the Lorentz force remains insignificant up to moderate values of magnetic field as far as dust dynamics is concerned. In this work, we try to show how the anisotropic magnetized wake influences the self-diffusion of dusty plasma even in this regime of magnetic field. The uniqueness of the present work is that we have used modified effective interaction potential while performing Langevin dynamics simulation, and this helps us to see the effect even for small to moderate values of magnetic field on dust dynamics. In the present work, we have discussed in detail the effect of magnetized wake on diffusion and phase behavior of a strongly coupled 3D dusty plasma system using Langevin dynamics simulation. Several important and novel features can be extracted from the present study. The observations can be summarized as follows.

- (1) For a range of normalized ion flow velocity ( $M$ ) lying between 1.0 and 1.2, the attractive wake potential is predominant and the dust ensemble exhibits superdiffusion.

- (2) Superdiffusion is also seen when magnetic field is increased beyond 0.09 T for suitable values of the Mach number in the supersonic regime.
- (3) The dust ensemble shows subdiffusion when the effective potential is Yukawa dominant and superdiffusion when it is wake dominant. The magnetized wake plays a crucial role in driving the system from subdiffusion to superdiffusion.
- (4) Both cross field ( $D_{\perp}$ ) and parallel ( $D_{\parallel}$ ) diffusion coefficients are sensitive to magnetic field, even when the field strength is weak. The nature of dependence of the perpendicular ( $D_{\perp}$ ) and parallel ( $D_{\parallel}$ ) diffusion coefficients on  $B$  depends on several factors like state of the system, ion flow velocity, and effective interaction potential. A novel regime of dependence of cross-field diffusion coefficient  $D_{\perp}$  as  $B^{\gamma}$  with  $\gamma > 2$  is observed for ultra-low magnetic field  $B$  ( $< 0.01$  T). On the other hand, combined effect of Lorentz force and wake potential lead the system to exhibit  $B^{-2}$  variation for relatively large magnetic field ( $> 0.09$  T).

## DATA AVAILABILITY

The data that support the findings of this study are available from the corresponding author upon reasonable request.

## REFERENCES

- <sup>1</sup>M. Nambu, S. V. Vladimirov, and P. K. Shukla, *Phys. Lett. A* **203**, 40–42 (1995).
- <sup>2</sup>M. Salimullah, P. Shukla, M. Nambu, H. Nitta, O. Ishihara, and A. Rizwan, *Phys. Plasmas* **10**, 3047–3050 (2003).
- <sup>3</sup>P. Bezbaruah and N. Das, *Eur. Phys. J. D* **71**, 114 (2017).
- <sup>4</sup>S. Bhattacharjee and N. Das, *Phys. Plasmas* **19**, 103707 (2012).
- <sup>5</sup>A. Melzer, V. Schweigert, and A. Piel, *Phys. Rev. Lett.* **83**, 3194 (1999).
- <sup>6</sup>W. J. Miloch, H. Jung, D. Darian, F. Greiner, M. Mortensen, and A. Piel, *New J. Phys.* **20**, 073027 (2018).
- <sup>7</sup>P. Ludwig, H. Kählert, and M. Bonitz, *Plasma Phys. Controlled Fusion* **54**, 045011 (2012).
- <sup>8</sup>E. Thomas, Jr., B. Lynch, U. Konopka, R. L. Merlino, and M. Rosenberg, *Phys. Plasmas* **22**, 030701 (2015).
- <sup>9</sup>L.-J. Hou, A. Piel, and P. Shukla, *Phys. Rev. Lett.* **102**, 085002 (2009).
- <sup>10</sup>T. Ott and M. Bonitz, *Phys. Rev. Lett.* **103**, 195001 (2009).
- <sup>11</sup>P. Bezbaruah and N. Das, *Phys. Plasmas* **25**, 053708 (2018).
- <sup>12</sup>M. Begum and N. Das, *Eur. Phys. J. Plus* **131**, 1–12 (2016).
- <sup>13</sup>Y. Feng, J. Goree, B. Liu, T. Intrator, and M. Murillo, *Phys. Rev. E* **90**, 013105 (2014).
- <sup>14</sup>P. Hartmann, J. C. Reyes, E. G. Kostadinova, L. S. Matthews, T. W. Hyde, R. U. Masheyeva, K. N. Dzhamagulova, T. S. Ramazanov, T. Ott, H. Kählert *et al.*, *Phys. Rev. E* **99**, 013203 (2019).
- <sup>15</sup>S. Nunomura, D. Samsonov, S. Zhdanov, and G. Morfill, *Phys. Rev. Lett.* **96**, 015003 (2006).
- <sup>16</sup>S. A. Khrapak, O. S. Vaulina, and G. E. Morfill, *Phys. Plasmas* **19**, 034503 (2012).
- <sup>17</sup>H. Ohta and S. Hamaguchi, *Phys. Plasmas* **7**, 4506–4514 (2000).
- <sup>18</sup>T. Ott and M. Bonitz, *Phys. Rev. Lett.* **107**, 135003 (2011).
- <sup>19</sup>T. Ott, M. Bonitz, Z. Donkó, and P. Hartmann, *Phys. Rev. E* **78**, 026409 (2008).
- <sup>20</sup>B. Liu and J. Goree, *Phys. Rev. Lett.* **100**, 055003 (2008).
- <sup>21</sup>J. Carstensen, F. Greiner, and A. Piel, *Phys. Rev. Lett.* **109**, 135001 (2012).
- <sup>22</sup>J. Allen, *Phys. Plasmas* **14**, 094704–094704 (2007).
- <sup>23</sup>M. Nambu, M. Salimullah, and R. Bingham, *Phys. Rev. E* **63**, 056403 (2001).
- <sup>24</sup>D. C. Rapaport, *The Art of Molecular Dynamics Simulation* (Cambridge University Press, 2004).
- <sup>25</sup>V. Fortov, A. Ivlev, S. Khrapak, A. Khrapak, and G. Morfill, *Phys. Rep.* **421**, 1–103 (2005).